DOI: 10.63527/1607-8829-2022-2-5-23

L.M. Vykhor, *DSc (Phys-Math)* [1]
P.V. Gorskyi, *DSc (Phys-Math)* [1,2]
V.V. Lysko, *Cand.Sc (Phys-Math)* [1,2]

[1]Institute of Thermoelectricity of the NAS and MES of Ukraine,
1, Nauky str., Chernivtsi, 58029, Ukraine;
[2]Yuriy Fedkovych Chernivtsi National University,
2, Kotsiubynsky str., Chernivtsi, 58012, Ukraine
e-mail: anatych@gmail.com

METHODS FOR MEASURING CONTACT RESISTANCES OF "METAL – THERMOELECTRIC MATERIAL" STRUCTURES (PART 1)

An overview of existing methods for measuring electrical contact resistance is presented. An analysis of their accuracy, advantages and disadvantages, as well as the possibilities of using them in thermoelectricity for the study and optimization of "metal – thermoelectric material" structures is conducted. Bibl. 11, Figs 14.

Key words: electrical contact resistance, measurement, accuracy, thermoelectric power converters.

Introduction

Reducing the cost of manufacturing thermoelectric power converters is a pressing issue in thermoelectricity. Solving this issue will significantly increase the competitiveness of both cooling and generating thermoelectric modules and expand the areas of their practical use.

In particular, the use of thermoelectricity for waste heat recovery is important. Almost all technological processes in industry, as well as the production of electrical energy, are associated with the use of fuels, including nuclear, to produce thermal energy. Most of this energy in industry, after the implementation of technological processes, is dissipated into the environment by gaseous or liquid heat carriers.

In heat engines, only 25 – 40 % of thermal energy is converted into mechanical energy. The remaining more than 50 % is given to the environment, which leads to its thermal pollution and disruption of the Earth's heat balance. This thermal power can be converted into electrical energy. The use of thermoelectric recuperators allows to extract from this heat as much electrical energy as all nuclear power plants generate. Thus, thermoelectric recuperators can become an important factor in the overall environmental improvement, and therefore are important for the interests of the human community.

At the same time, the main obstacle to the widespread practical use of thermoelectricity for the recovery of waste heat is the high cost of thermoelectric energy converters, the largest share of which is the cost of thermoelectric material. The cost of thermoelectric energy converters can be reduced by tens of times and approach the required for wide practical applications due to their miniaturization.

However, attempts to create miniature modules encounter the growing influence of contact resistances, which cause a catastrophic decrease in the quality of the modules.

The development and optimization of technologies for creating contact resistances necessary to

meet practical needs is carried out experimentally by studying the influence of various technological factors on the value of contact resistance. The latter is possible only if reliable methods and equipment for measuring contact resistances are available.

The purpose of this work is to analyze existing methods and equipment for determining the values of contact resistances and the possibilities of their use for the study and optimization of "metal – thermoelectric material" structures.

1. Methods for measuring electrical contact resistance

1.1 Methods used in microelectronics

The most modern methods for measuring electrical contact resistance include the Cox-Streck method, the transmission line method, the Kelvin method, and the boundary probing method. These methods are successfully used in microelectronics [1 – 10].

The authors of [1] proposed contacts made of silver alloy with indium and germanium for *n*-type gallium arsenide and contacts made of silver alloy with indium and zinc for *p*-type gallium arsenide. Depending on the specific resistance of gallium arsenide, the resistance of such contacts is from 10^{-4} to 10^{-3} Ohm·cm^2.

In [2], it is shown that the contact resistance is significantly affected by the technology of cleaning the semiconductor surface. In particular, sputtering cleaning instead of chemical etching significantly reduces the contact resistance.

In [3], various methods for measuring contact resistance and common sources of error are discussed. A number of methods are described, in particular the transmission line method. The results of measuring contact resistances for aluminum-silicon contacts over a wide range of doping levels of the silicon surface layer are presented and discussed.

In [4], a method for separating the contact resistance from the resistance of a bulk sample was proposed. This method is based on measuring the angular dependence of the geometric magnetoresistance. Its efficiency was tested on the Gunn diodes. The error is less than 0.5 % of the total resistance of the device.

In [5], a setup for simultaneous measurement of electrical and thermal contact resistances between metals is described. It allows measuring electrical contact resistance with an error of 0.003 % and thermal contact resistance with an error of 4.4 %. The measurement results for real contacts are in good agreement with theoretical calculations available in the literature.

In [6], a device for measuring electrical contact resistance is described. It can be used to measure contact resistances of the order of 10 μΩ. It uses a current through the contact of about 1 mA, which prevents the formation of an electric arc.

In [7], it is indicated that the measurement of the contact resistance of a "metal-high-resistance semiconductor" is associated with significant difficulties, so that the error can reach five orders of magnitude. It is shown that the transmission line method is inapplicable if the contact resistance is less than 10^{-3}Ω·cm^2.

In [8], a device was developed for measuring the contact resistance between metal wafers as a function of pressure and the corresponding dependence for a pair of copper wafers was investigated.

In [9], the electrical contact resistance between contacts made of *Fe-Cr* alloy and thermoelectric material $Ca_3Co_4O_9$ was measured. The maximum contact resistance obtained was $1.2\cdot10^{-7}$Ohm·cm^2.

The essence of the main methods for measuring contact resistance in microelectronics is presented in [10]. Methods for measuring contact resistance are divided into four categories:

1) two-contact two-terminal;
2) multi-contact two-terminal,
3) four-terminal,
4) six-terminal.

None of these methods are applicable to the measurement of surface resistivity ρ_i. Instead, the specific contact resistance ρ_c is determined, which is not the actual surface resistance of the metal-semiconductor interface, but it is a practically applicable numerical characteristic that describes the real contact. From this point of view, comparing theory and experiment is quite difficult, since theory cannot accurately predict ρ_c, and experimentally it is difficult to accurately measure ρ_i. It is often difficult even to unambiguously measure ρ_c. We will limit ourselves to discussing experimental techniques.

1.1.1 Two-contact two-terminal method

This method is the earliest. Its accuracy is rather questionable and it is rarely used. Its simplest schematic implementation is shown in Fig. 1.

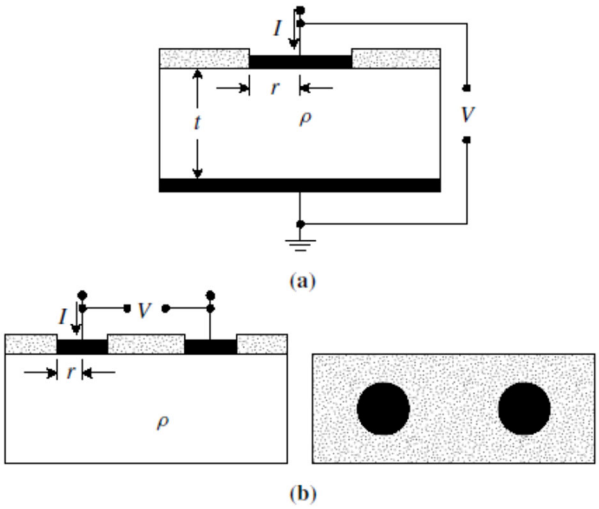

Fig. 1. Vertical two-terminal structure (a) and surface two-terminal structure (b) for measuring contact resistance [10].

For a homogeneous semiconductor with resistivity ρ and thickness t, the total resistance $R_t = V/I$ measured according to diagram (a) by passing current I through the sample with determination of the voltage V between the contacts is equal to:

$$R_T = R_c + R_{sb} + R_{cb} + R_p . \quad (1)$$

When measuring according to diagram (b), instead of (1), the following relation is used:

$$R_T = 2R_c + 2R_{sb} + 2R_p . \quad (2)$$

In these formulae, R_c – the contact resistance of the upper contact, R_{sb} – the spreading resistance directly under the contact, R_{cb} – the contact resistance of the lower contact, R_p – the resistance of the probe or wire. Typically, the lower contact has a large area, and, therefore, a relatively low associated contact resistance. Therefore, the contact resistance of the lower contact is often neglected. Similarly,

the probe resistance is also assumed to be low.

The spreading resistance of a flat non-penetrating contact of circular shape with radius r on the surface of a semiconductor with resistivity ρ and thickness t is equal to:

$$R_{sp} = \frac{\rho}{2\pi r}\operatorname{arctg}\left(2t/r\right) \tag{3}$$

In the case $2t >> r$ the following relation is valid:

$$R_{sp} = \frac{C\rho}{4r}. \tag{4}$$

In this formula, C is the correction factor, which depends on ρ, r and current distribution. For widely spaced contacts, as in diagram (b), located on a homogeneously doped semi-confined substrate, $C = 1$. If the current flows vertically into the upper contact, as in diagram (a), then the contact resistance is:

$$R_c = \rho_c / A_c = \rho_c / \pi r^2 \tag{5}$$

Relation (1) shows that with low R_{cb} and R_p the contact resistance will be the difference between the total resistance and spreading resistance. But the spreading resistance cannot be measured independently. Therefore, even small errors in the spreading resistance will lead to significant errors in the value of contact resistance. Hence, the two-terminal method works best when $R_{sp} << R_c$, that is, in the case of contacts of small radius.

A modification of the two-terminal method is the use of upper contacts of different diameters. Therefore, from the known values of R_T it is possible to determine and plot the dependence of R_c on $1/A_c$ and to determine ρ_c by the slope of the corresponding plot. Alternatively, it is possible to plot the total resistance as a function of $1/r$. Using contacts of different diameters, from the shape of the curve it is possible to determine whether the data are anomalous.

The two-terminal method is most often implemented using the horizontal (surface) structure shown in Fig. 2.

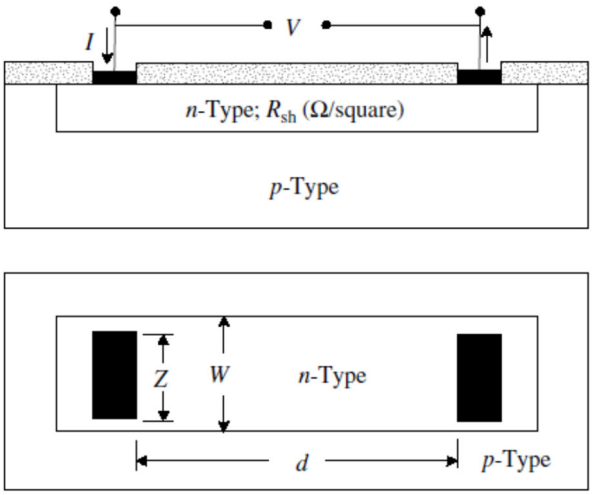

Fig. 2. Surface (horizontal) structure for implementing the two-terminal method of measuring contact resistance in section and plan view [10].

It differs from the structure shown in Fig. 1*b* in that the current is limited by an n-type island. The test structure consists of two contacts separated by a distance. In order to limit the current, the area in which the contacts are located must be isolated from the rest of the substrate by doping or diffusion so that, for example, an n-type region is formed in the p-substrate by planar technology or by chemical etching of the region surrounding the island, leaving a "mesa". The island in this example has a width W and ideally the contacts should have the same width. However, this is difficult to do, so the width of the contacts Z usually differs from W . In this case, the analysis is complicated by the horizontal flow of current, the increase in its density near the contacts and the geometry of the sample. For the geometry shown in Fig. 2, the total resistance is:

$$R_T = R_{sh} d / W + R_d + R_w + 2R_c \,. \tag{6}$$

In this formula, R_{sh} – the surface resistance of the n-layer, R_d – the correction for the current change near the contact, R_w – the correction for the contact width, if $Z < W$. The expressions for the resistances appearing in formula (6), are given in [10].

For the case of many contacts, the so-called "*contact chain method*" is used, the diagram of which is shown in Fig. 3.

In this diagram, the total resistance between each pair of contacts is defined as the sum of the semiconductor resistance, the contact resistance, and the metal resistance. The semiconductor resistance is calculated from the known surface resistance and the geometry of the circuit. Subtracting the semiconductor resistance from the total resistance gives the total contact resistance. The contact resistance of each contact is obtained by dividing the result by twice the number of contacts.

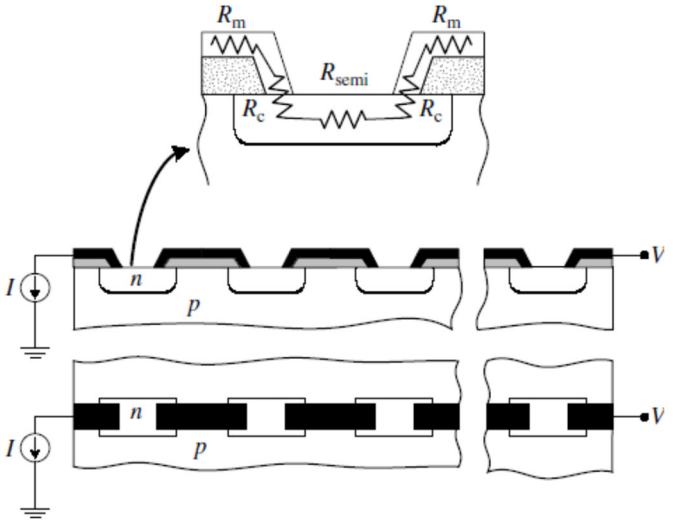

Fig. 3. Diagram of the "contact chain" method and images of the test structure in plan and section [10].

In this diagram, the total resistance between each pair of contacts is defined as the sum of the semiconductor resistance, the contact resistance, and the metal resistance. The semiconductor resistance is calculated from the known surface resistance and the geometry of the circuit. Subtracting the semiconductor resistance from the total resistance gives the total contact resistance. The contact resistance of each contact is obtained by dividing the result by twice the number of contacts. For a contact chain consisting of *N* islands and *2N* contacts of width *W*, separated by a distance, and neglecting the metal resistance, the following relation is valid:

$$R_T = \frac{NR_{sh}d}{W} + 2NR_c . \quad (7)$$

This method is too rough for accurate assessment of contact resistance. However, it is often used for process control.

1.1.2 Multi-contact two-terminal method

The diagram of the method is shown in Fig. 4, the test structure for its implementation is shown in Fig. 5.

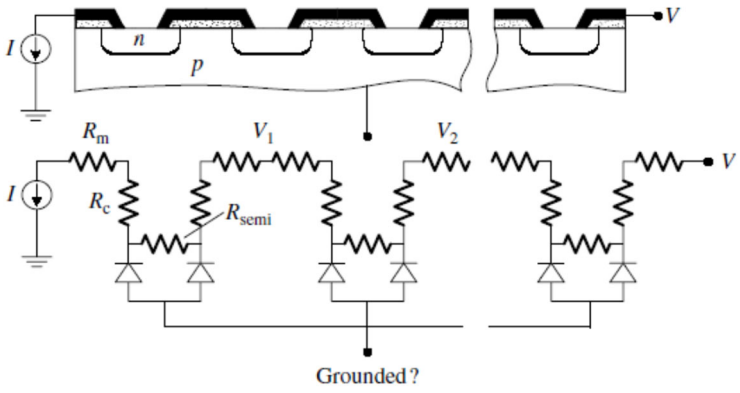

Fig. 4. Diagram of multi-contact-two-terminal method [10].

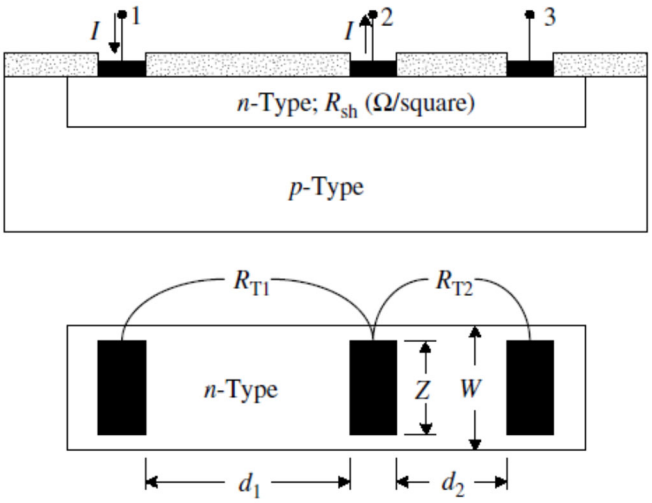

Fig. 5. Test structure for the implementation of multi-contact two-terminal method [10].

This method was developed to overcome the shortcomings of the two-contact two-terminal method. It creates three identical contacts to the semiconductor, separated by distances d_1 and d_2. Assuming that the contact resistances of all three contacts are the same, the total resistance can be determined as follows:

$$R_{Ti} = \frac{R_{sh}d_i}{W} + 2R_c . \quad (8)$$

Therefore, substituting $i = 1,2$ and solving the corresponding system of equations for R_c, we obtain:

$$R_c = \frac{R_{T_2} d_1 - R_{T_1} d_2}{2(d_1 - d_2)}. \quad (9)$$

This test structure does not have the uncertainties of a simple two-terminal structure, since it is not necessary to know the volume and surface resistance of the semiconductor. The assumption that the contact resistances of all three contacts are the same is somewhat questionable, but it is justified if the sample is not very large. The contact resistance is determined by the difference of two large values. This can be difficult, especially for contacts with low resistance. The determination of distances d_1 and d_2 is an additional source of inaccuracies. Incidentally, this method can also give a negative value for the contact resistance.

The structure in Fig. 5 allows only the contact resistance to be determined. The specific contact resistance cannot be directly determined from two resistance measurements. The determination requires a more detailed assessment of the current distribution in and outside the horizontal contact region. Early studies of the two-dimensional current distribution in diffusion resistors by Kennedy and Marley showed that there is current concentration at the contacts. Analysis under the assumption of zero contact resistance showed that only a portion of the contact length is active in the transfer of current from the semiconductor to the metal and vice versa. This portion was found to be approximately equal to the thickness of the diffusion semiconductor layer.

Let us now consider some test structures for measuring contact resistance, which are shown in Fig. 6.

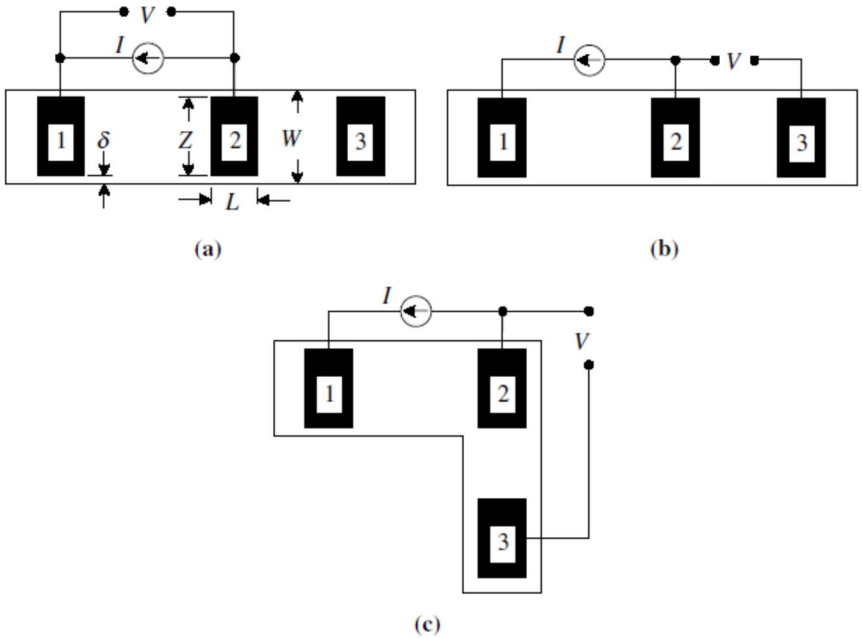

Fig. 6. Test structures for measuring contact resistance: a) conventional; b) for measuring contact resistance of the end contact; c) Kelvin test structure of the "cross bridge" type [10].

In all of these structures, the current flows from contact 1 to contact 2. In the test structure for implementing the line transmission method shown in Fig. 6a, which is also called the *structure for measuring the front contact resistance*, the voltage is measured between the same contacts as the current. In the test structure shown in Fig. 6b, the voltage is measured between contacts 2 and 3. In the test structure for measuring contact resistance by the Kelvin method (Fig. 6c), which is considered to be one

of the most accurate, the voltage is measured at right angles to the current.

Let us now consider the expressions for the resistances in these circuits. In diagram 6a, the resistance of the front contact is:

$$R_{cf} = V/I = \frac{\sqrt{R_{sh}\rho_c}}{Z}\operatorname{cth}\left(L/L_T\right) = \frac{\rho_c}{L_T Z}\operatorname{cth}\left(L/L_T\right), \tag{10}$$

if $Z = W$. If the sample is wider than the contact, then formula (10) is only approximate.

It is usually considered that $R_{cf} = R_c$. The general formula (10) allows for a number of simplifications.

For instance, if $L < 0.5L_T$,then $\operatorname{cth}\left(L/L_T\right) \approx L_T/L$, hence,

$$R_c = \frac{\rho_c}{LZ}. \tag{11}$$

If $L > 1.5L_T$, then $\operatorname{cth}\left(L/L_T\right) \approx 1$, hence

$$R_c = \frac{\rho_c}{L_T Z}. \tag{12}$$

In the first case, the true contact area coincides with its effective area. However, in the second case, the effective contact area is smaller than the true one. This leads to a number of important consequences. For example, consider a structure with a surface resistance of 20 Ohm/sq and a contact resistance of 10^{-7} Ohm·cm^2. In this case, the "characteristic transmission length" is 0.7 μm. For a contact 10 μm long and 50 μm wide, the true contact area is $5\cdot10^{-6}$ cm^2. However, the effective contact area is only $3.5\cdot10^{-7}$ cm^2.

Thus, the current density in the contact becomes 14 times higher than in the case when the entire contact is active. This increase in the current density in the contact causes problems associated with contact degradation. The reduced contact area burns out in extreme cases and the active area of the contact gradually shifts until it is completely destroyed.

The contact model shown in Fig. 6 may be oversimplified in the case of a series of contacts. For example, in the case of alloy contacts, the contact region consists of the metal, the alloy region, and an adjacent semiconductor layer. Contacts obtained by sputtering a metal onto a thin layer of a narrow-gap or wide-gap semiconductor also fall into this category. This requires a more complex transmission line model, and a symmetrical layer model. Then the corresponding equations become significantly more complicated.

When voltage is measured between contacts 2 and 3, while current flows between contacts 1 and 2 (Fig. 6b), the corresponding contact resistance is:

$$R_{ce} = V/I = \frac{\sqrt{R_{sh}\rho_c}}{Z\operatorname{sh}\left(L/L_T\right)} = \frac{\rho_c}{L_T Z\operatorname{sh}\left(L/L_T\right)}. \tag{13}$$

The measurement of contact end resistance can be used to determine the specific contact resistance by measuring R_{ce} and iterating the relation (13). In the case of short contacts, R_{ce} is sensitive to changes in the contact length, so the error in the determination of L limits the accuracy of the method. For long contacts R_{ce} becomes small and the accuracy of its determination is limited by the error of the

instruments. This can be seen by constructing the relation

$$\frac{R_{ce}}{R_{cf}} = \frac{1}{\mathrm{ch}\left(L/L_T\right)}, \tag{14}$$

which becomes very small for $L >> L_T$.

For the case of the Kelvin test structure (Fig. 6c), contact 3 is located away from contact line 1-2. Therefore, the measured voltage is the average value of the potential along the length of the contact, i.e.:

$$V = L^{-1}\int_0^L V\left(x\right)dx, \tag{15}$$

Integrating, we get:

$$R_c = V\Big/ I = \frac{\rho_c}{LZ}, \tag{16}$$

Equation (13) assumes that the width of contact Z is equal to the width of the semiconductor layer. This is rarely realized in practice. Usually $Z < W$. Experiments at Z=5 μm and W in the range from 10 to 60 μm show that the method of measuring the resistance of the end of the contact gives a falsely large contact resistance. The error increases if ρ_c decreases. Or if R_{sh} increases.

The source of error is the potential difference between the front and rear edges of the contact, as a result of which the current can flow around the edges of the contacts. The measured resistance is proportional to the surface resistance and is insensitive to the contact resistance for large δ. For the validity of a simple one-dimensional theory, the test structure must satisfy the conditions $L \le L_T, Z >> L$ and $\delta << Z$. The "one-dimensional" analysis is not suitable if the specified conditions are not satisfied. However, an accurate determination of ρ_c is possible if the numerical calculations (simulation) are properly adjusted to the measurement data.

The problem associated with $W \neq Z$ can be prevented by using a circular (annular) test structure consisting of a leading inner region of radius L, a gap of width *d*, and an inner contact region. The leading regions are usually metallic, and the gap width varies from a few microns to tens of microns. The structure is shown in Fig. 7.

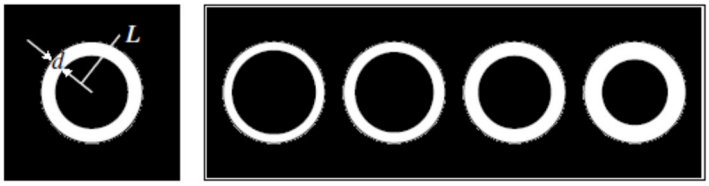

Fig. 7. A separate element of the circular structure (a) and the structure as a whole (b). Black areas – metal [10].

If the surface resistances of the semiconductor layer under the metal and in the gap are the same, then the following expression is valid for the total resistance between the external and internal contacts:

$$R_T = \frac{R_{sh}}{2\pi}\left[\frac{L_T}{L}\frac{I_0\left(L/L_T\right)}{I_1\left(L/L_T\right)} + \frac{L_T}{L+d}\frac{K_0\left(L/L_T\right)}{K_1\left(L/L_T\right)} + \ln\left(1+\frac{d}{L}\right)\right] \tag{17}$$

In these formulae, $I_m(z)$ and $K_m(z)-$ Bessel functions of imaginary argument and modified Bessel functions of corresponding indices.

For the circular transmission line test structure shown in Fig. 7, under the condition $L >> 4L_T$ the ratios I_0/I_1 and K_0/K_1 tend to unity, and, hence, expression (17) is simplified:

$$R_T = \frac{R_{sh}}{2\pi}\left[\frac{L_T}{L} + \frac{L_T}{L+d} + \ln\left(1+\frac{d}{L}\right)\right] \tag{18}$$

If, in addition, $L >> d$, the expression (25) takes on the form:

$$R_T = \frac{R_{sh}C}{2\pi L}\left(d + 2L_T\right), \tag{19}$$

where

$$C = \frac{L}{d}\ln\left(1+\frac{d}{L}\right) \tag{20}$$

For practical radii of about 200 μm and gap widths in the range of 5 – 50 μm, a correction factor d/L is needed to compensate for the difference between the results of the linear transmission line method and the consideration according to the circular diagram in order to obtain a linear smoothing of the experimental data. Without the correction factor, the specific contact resistance is underestimated. Similar to the case of the linear structure, the corrected data allow the characteristic transmission length and hence the specific contact resistance to be estimated.

The circular test structure has one significant advantage. It is that there is no need to isolate the semiconductor layer during measurements, since current can only flow from the centre contact to the surrounding contact. In a linear test structure, for the transmission line method, current can flow from contact to contact through the area outside the test structure, if it is not isolated. The circular test structure with four metal contacts is very similar to the Kelvin cross-bridge resistor discussed earlier (see Fig. 6 *c*).

Equations (10) and (13) were obtained on the assumption that $\rho_c > 0.2R_{sh}t^2$, where t – layer thickness. For $R_{sh} = 20\,\text{Ohm/sq}$ and $t = 1\,\mu\text{m}$ this condition leads to inequality $\rho_c > 4\times10^{-8}\,\text{Ohm·cm}^2$. The transmission line method must be modified if this condition is not satisfied, which is verified by experiments and simulations. However, most contact resistances are much larger, so the transmission line method is suitable.

The difficulty in deciding where to measure the voltage in the diagrams in Fig. 6 led to the emergence of the test structure shown in Fig. 8 and the corresponding "transmission length method" proposed by Shockley.

The structure for implementing this method is very similar to the structure shown in Fig. 2, but contains more than 3 contacts. The two contacts at the ends of the test structure serve to allow current to enter and exit the original "ladder" structure, and the voltage is measured between one of the large contacts and each of the successive narrow contacts as in Fig. 8a. Later, the structure shown in Fig. 8b was proposed, in which the voltage is measured between adjacent contacts.

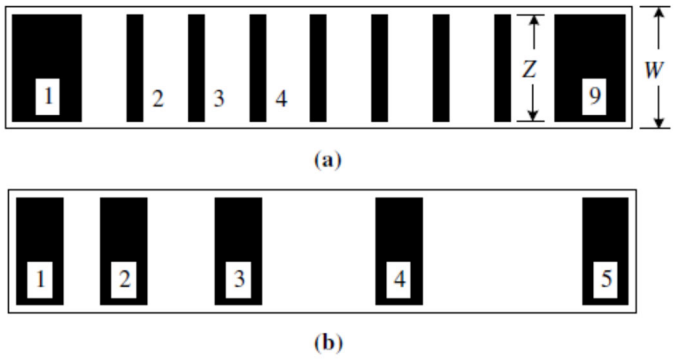

Fig. 8. Test structures for implementing the "transmission length method" [10].

The structure in Fig. 8b has certain advantages over the structure shown in Fig. 8a. If the voltage in the "ladder" structure is measured, for example, between contacts 1 and 4, then there is a current disturbance due to the presence of contacts 2 and 3. The influence of contacts 2 and 3 depends on the "characteristic transmission length L_T and contact length L. If $L << L_T$, the current does not penetrate noticeably into contact 2 and, therefore, contacts 2 and 3 do not affect the measurement results. If, however, $L >> L_T$, current flows in the metal and the contact can be imagined as two contacts of length L_T, which are located in a metal conductor Shunting the current by metal strips obviously affects the measured voltage value, and therefore the resistance. From this point of view, the structure in Fig. 8b is better, since it has a "pure" semiconductor between every two contacts (in the sense that the corresponding gap is sufficient for the current not to penetrate into the adjacent contact).

For contacts that satisfy the condition $L \geq 1.5L_T$, the following expression is valid for the measured resistance of the front contact:

$$R_T = R_{sh} d \Big/ Z + 2R_c \approx \frac{R_{sh}}{Z}\left(d + 2L_T\right), \tag{21}$$

where we used the same approximation that leads from formula (10) to formula (12).

The dependence of the measured contact resistance on d is shown in Fig. 9.

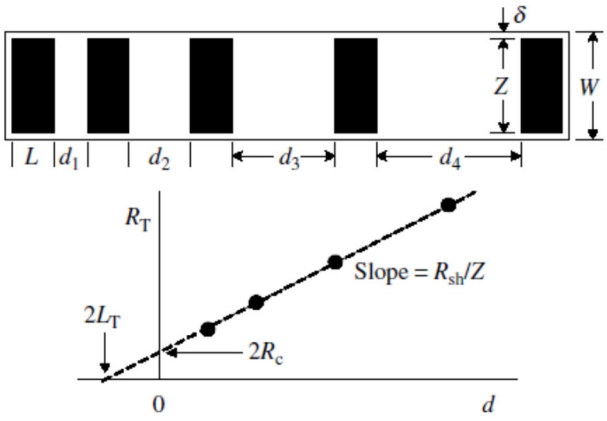

Fig. 9. Test structure for implementing the "characteristic transmission length" method and the dependence of the measured total resistance on d [10].

The slope of the line $\Delta d/d = R_{sh}/Z$ allows one to determine the surface resistance R_{sh}, if the contact width Z is known from independent measurements. The intersection of the plot with the vertical axis, given $d = 0$ allows one to determine the total contact resistance. The intersection of the plot with the horizontal axis, given $R_T = 0$ allows one to determine the "characteristic transmission length", and, hence, the specific contact resistance, since the surface resistance R_{sh} is known from the slope of the line. Thus, this method gives a complete characterization of the contact, including the surface resistance of the semiconductor layer, the total contact resistance and the specific contact resistance.

This method is usually used to measure contact resistance, but it has its own problems. For example, the point of intersection of the plot with the horizontal axis is not always clearly defined, which leads to an incorrect value of L_T, and, hence, of ρ_c. However, a more serious problem is the uncertainty of the surface resistance of the semiconductor layer under the contacts. Eq. (21) is valid assuming the same surface resistance of the semiconductor layer under the contacts and between them. However, these resistances can differ from each other due to effects associated with the formation of the contact. This is true for alloy and "silicide" contacts, when the semiconductor region under the contact is modified in the process of obtaining the contact. In this case, the following expressions are valid for the resistance of the front edge of the contact and the total resistance:

$$R_{cf} = \frac{\rho_c}{L_{Tk} Z} \operatorname{cth}\left(L/L_{Tk}\right). \tag{22}$$

$$R_T = \frac{R_{sh} d}{Z} + 2R_k \approx \frac{R_{sh} d}{Z} + \frac{2R_{sk} L_{Tk}}{Z} = \frac{R_{sh}}{Z}\left[d + 2\left(R_{sk}/R_{sh}\right)L_{Tk}\right]. \tag{23}$$

In formula (23), R_{sk} – the modified surface resistance of semiconductor layer under the contact, $L_{Tk} = \sqrt{\rho_c / R_{sk}}$. The slope of the dependence of R_T on d, as before, is determined by R_{sh}/Z and the point of intersection with the vertical axis gives $2R_c$. However, the point of intersection with the horizontal axis gives $2\left(R_{sk}/R_{sh}\right)L_{Tk}$, therefore, the specific contact resistance is now impossible to determine, since R_{sk} is unknown. Nevertheless, determining R_{cf} by the method of "characteristic transmission length" and R_{ce} by "contact end resistance" method, where:

$$R_{ce} = \frac{\sqrt{R_{sk}\rho_c}}{Z \operatorname{sh}\left(L/L_{Tk}\right)} = \frac{\rho_c}{Z L_{Tk} \operatorname{sh}\left(L/L_{Tk}\right)}; \frac{R_{ce}}{R_{cf}} = \frac{1}{\operatorname{ch}\left(L/L_{Tk}\right)}. \tag{24}$$

one can determine L_{Tk} and ρ_c. Thus, it becomes possible to determine the contact resistance and specific contact resistance in addition to the resistance of the surface layer of the semiconductor between and under the contacts. It is also possible to separate R_{sh} from R_{sk} by etching the semiconductor between the contacts.

The determination of electrical parameters of contacts by the transmission line method is based on the assumption that the electrical and geometric parameters of the contacts are uniform across the sample cross-section. However, these parameters are usually scattered across the chip (wafer). Statistical simulation shows that the usual data acquisition procedure can lead to errors even if there are no errors in the measurement of electrical and geometric parameters. For the case of short contacts ($L < L_T$) ρ_c can be determined, despite the scattering of other parameters, whereas the error in the determination of

R_{sk} and R_{sh} occurs only when ρ_c is scattered across the wafer. In the case of long contacts, the found values of ρ_c and R_{sk} have an error when there is a measurement error. The best results are obtained when $L \geq 2L_T$. If a wafer has a non-uniform distribution of electrical parameters with fluctuations of 10-30%, then the error in the determination of ρ_c and R_{sk} can reach 100-1000%. The use of more than one test structure makes it possible to reduce the errors.

1.1.3 Four-terminal method for measuring contact resistance

The methods of measuring contact resistance considered earlier require knowledge of the value of the specific or surface resistance of the semiconductor layer. However, such methods of measuring R_c and ρ_c that would minimize the contribution of the resistance of the semiconductor layer or eliminate it altogether are preferable. The measurement method that is most suitable for this purpose is the Kelvin method, which is based on the Kelvin structure with "crossing bridges". This test structure was first used in 1972, but it was not until the early 1980s that it was seriously evaluated. In principle, this method allows the actual contact resistance to be measured, uncorrupted by the resistances of the semiconductor and metal. The measurement principle is illustrated in Fig. 10.

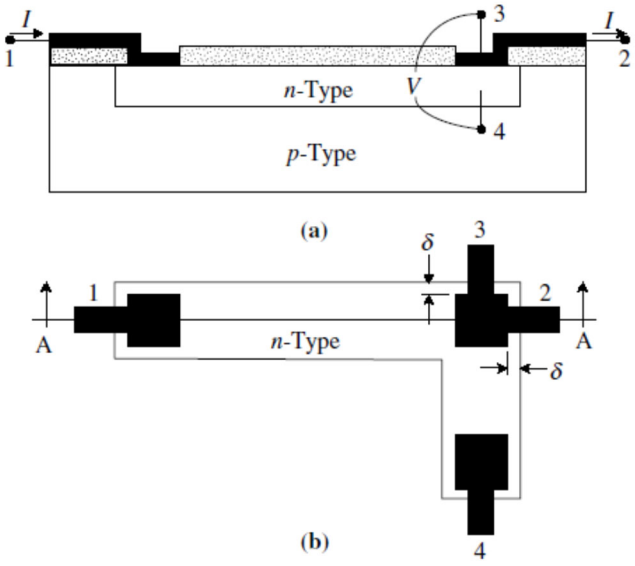

Fig. 10. Kelvin test structure in section A-A and in plan [10].

Current is passed between contacts 1 and 2, and voltage is measured between contacts 3 and 4. There are three voltage jumps between contacts 1 and 2. The first is between wafer 1 and the semiconductor layer, the second is along the surface of the semiconductor layer, and the third is between the n-layer and wafer 2/3. The high input impedance of the voltmeter causes very little current between contacts 3 and 4. Therefore, the potential at contact 4 is the same as the potential of the n-region directly below wafer 2/3, as illustrated in Fig. 10a by placing point 4 directly below contact 3. Thus, the measured voltage V_{34} is entirely due to the jump at the metal-semiconductor contact. The contact resistance is then:

$$R_c = V_{34}/I\,, \tag{25}$$

therefore, the specific contact resistance is equal to

$$\rho_c = R_c A_c , \tag{26}$$

where A_c – contact area.

This method is considered to be the most accurate, but the relation (26) does not always agree with the experimental data. The specific contact resistance calculated in accordance with (26) is an imaginary contact resistance distorted by the surface current concentration in the case when the contact windows are smaller than the diffusion gap, denoted as δ in Fig. 10. The curvature of the contact window to the diffusion layer and the horizontal diffusion of the dopant are taken into account under the condition $\delta > 0$. The ideal case $\delta = 0$ is illustrated in Fig. 11a. In a real contact, part of the current, shown by the arrows in Fig. 11b, flows around the metal contact. In the ideal case, when $\delta = 0$, the potential jump $V_{34} = IR_c$.

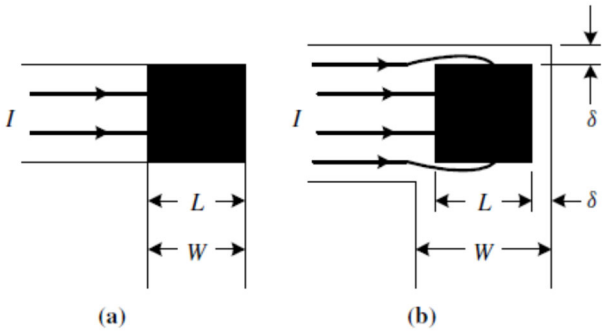

Fig. 11. Kelvin test structures: a) ideal; b) taking into account horizontal current flow around and under the contact [10].

In the case of $\delta \neq 0$ the horizontal current creates an additional voltage jump, which is included in V_{34} and leads to a higher value of the measured voltage. According to relation (26) ρ_c increases if the true contact area is used. The thus obtained value of ρ_c is known as the imaginary specific contact resistance. The error introduced by the above geometric factor is greater for lower values of ρ_c, and (or) higher R_{sh} and less for higher values of ρ_c, and (or) lower values of R_{sh}. The vertical voltage jump in the semiconductor, normal to the contact plane, is usually not taken into account, although it also introduces a correction.

1.1.4 Six-terminal method for measuring contact resistance

The diagram of the six-terminal method for measuring contact resistance is shown in Fig. 12.

The appropriate test structure is a four-terminal Kelvin test structure with two additional contacts to provide additional capabilities not available in the conventional Kelvin structure. This structure allows the determination of contact resistance, contact resistivity, contact start resistance, contact end resistance and semiconductor surface resistance. In the case of a conventional Kelvin structure, current is pumped between contacts 1 and 3 and voltage is measured between contacts 2 and 4. Then $R_c = V_{24}/I$, and, hence, $\rho_c = R_c/A_c$. The problems arising from consideration within the framework of a two-dimensional model remain for the six-terminal structure.

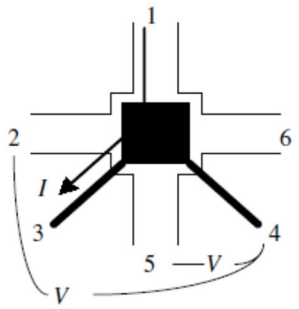

Fig. 12. The diagram of the six-terminal method for measuring contact resistance, allowing simultaneous determination of $R_c, R_{ce}, R_{cf}, R_{sk}$ *[10].*

To measure the resistance of the contact end in conformity with relation $R_{ce} = V_{54}/I$ current is passed between contacts 1 and 3, and voltage is measured between contacts 5 and 4. Given the contact resistance and the specific contact resistance known earlier, the surface resistance of the semiconductor under the contact can be determined through the resistances R_{ce} and R_{cf} from relations (10) and (24).

2. Measurement of electrical contact resistance in thermoelectricity

It is known that the influence of contact resistance on the efficiency of a thermoelectric device increases as it is miniaturized. Popular methods for measuring contact resistance in microelectronics are suitable for thin films, but cannot be directly transferred to the case of bulk TE materials. The authors of [11] propose a method for measuring contact resistance for the case of bulk TE materials by manufacturing and testing stacks of TE material wafers covered with metal using a traditional technological process for manufacturing thermoelectric devices. The thermoelectric figure of merit *Z* of the stack is used to isolate the contact resistance and reduce the sensitivity of the results to the resistance of the TE material. The advantage of this technique is that it reflects the real technological process of manufacturing TE devices and copies structures similar to real TE devices with maximum accuracy. The smallest values of the electrical contact resistance that were measured by this method at 300K were $1.1 \cdot 10^{-6}$ and $1.3 \cdot 10^{-6}$ Ω·cm^2 for n- and p-type materials, respectively. The measurement error for each sample is from 10 to 20%, which is acceptable when measuring contact resistances of the order of 10^{-6} Ω·cm^2.

The improved method for measuring contact resistance by thermoelectric figure of merit in cooling mode, described in [11], is as follows. It is known that the maximum cooling capacity of a thermocouple is defined as:

$$Q_{\max} = \frac{1}{2L}\left[\frac{\alpha^2 T_c^2}{(2\rho + 4\rho_c/L)} - k\Delta T\right]. \qquad (27)$$

In this formula, L – the length of the thermoelectric leg, α – the Seebeck coefficient, T_c – the cold junction temperature, ρ – the resistivity of the semiconductor, ρ_c – the contact resistance, k – the thermal conductivity, ΔT – the temperature difference. The influence of contact resistance on the performance of the refrigerator is considered to be significant when the leg lengths are 200 μm or less. Specific contact resistance is difficult to measure when it is less than 10^{-6} Ohm·cm^2. In order to

quantitatively evaluate the contact resistance on Bi_2Te_3, a stack structure simulating a real device was developed and applied. The technological process of manufacturing a stack-like structure was similar to that of a real thermoelectric cooler, so that the contact resistance was well reproduced. The stack-like structure was made of several wafers of thermoelectric material. The wafers were soldered together in a single process and cut into "cubes", as shown in Fig. 13.

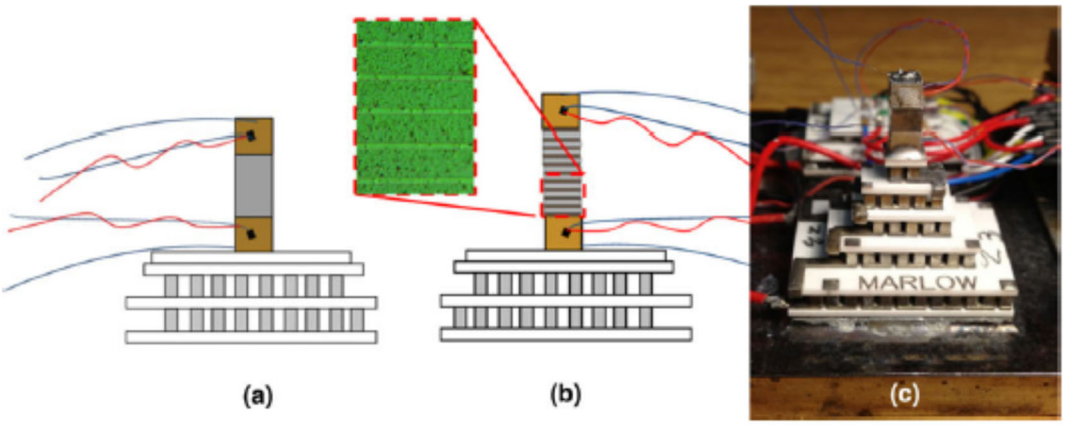

Fig. 13. Method of measuring contact resistance by the figure of merit [11]: a) – control sample; b) – stack-shaped structure; c) – general view of the measuring setup.

The process of sample manufacturing is shown in Fig. 14.

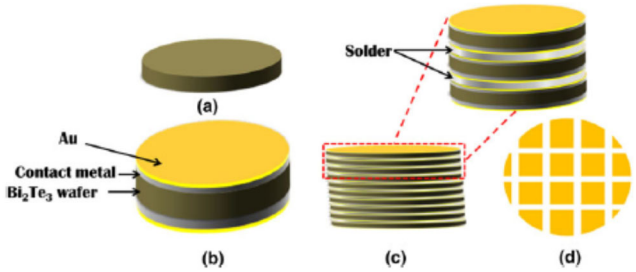

Fig. 14. Sequential stages of sample manufacturing process [11]: a) – single wafer after lapping; b) – wafer after etching and deposition of contact layer; c) – finished stack of 10 wafers after soldering; d) – stack of wafers cut into cubes.

The samples were manufactured as follows. First, the wafers were ground to a thickness of 250 µm. The composition of the TE materials was approximately as follows: *n*-type – $(Bi_2Te_3)_{0.9}(Bi_2Se_3)_{0.1}$, *p*-type – $(Sb_2Te_3)_{0.75\text{-}0.80}(Bi_2Te_3)_{0.2\text{-}0.25}$. After lapping, the wafers were subjected to surface treatment and metal deposition. Gold was deposited on the surface of the metal contacts to prevent surface oxidation and to ensure wetting with solder. After metal deposition, the wafers were placed in a special clamping device. Solder was applied manually using ceramic strips to ensure a flat and smooth surface. Then one wafer was placed on top of the other and carefully pressed. Excess solder was removed. The process continued until a stack of 10 plates was formed. Tin-antimony solder was used to form the stacks. After that, the finished stacks were inserted into the furnace. The uniformity of the solder and the reproducibility of the technological process of forming the stacks were checked by numerous tests. After that, the finished stacks were cut into squares with a side of 3.8 mm. Copper pads with conductive wires were soldered to the end of each stack. In order to produce control samples with the same thermoelectric properties, solid wafers 2.5 mm high were made from an adjacent piece of each

corresponding ingot. The control samples and stacks were placed in a figure of merit measurement setup and the thermoelectric properties were measured in the temperature range from 260 to 340 K.

The thermoelectric figure of merit was measured by the modified Harman method. The Seebeck coefficient α and the resistivity ρ were also measured. The measuring setup was calibrated to ensure a measurement error of no more than 2 %.

The essence of the measurement method is as follows. The figure of merit of the control sample is:

$$Z_{\text{control}} = \frac{\alpha^2 L}{k\left(\rho L + 2\rho_c\right)}. \tag{28}$$

At the same time, the figure of merit of the device in the form of a stack is equal to:

$$Z_{\text{stack}} = \frac{\alpha^2}{k\left(\rho + 2\rho_c / t\right)}. \tag{29}$$

It is clear that due to the small average distance t between the wafers in the stack the difference between Z_{control} and Z_{stack} can be made quite noticeable and, therefore, the accuracy of determining the specific contact resistance ρ_c is significantly increased. Dividing (28) by (29) and solving the resulting equation for ρ_c, we obtain:

$$\rho_c = \frac{\rho L}{2}\left(\frac{Z_{\text{ratio}} - 1}{Lt^{-1} - Z_{\text{ratio}}}\right). \tag{30}$$

In this formula,

$$Z_{\text{ratio}} = Z_{\text{control}} / Z_{\text{stack}}. \tag{31}$$

To improve accuracy, it is necessary to make several control samples and stacks and take the average values of the corresponding figures of merit measured by the modified Harman method.

The authors of [11] used averaging over 5 stacks and 3 control samples. Thus, in each experiment, averaging was performed over more than 100 interfaces. Due to the main contribution of contact resistance to the change in the figure of merit of the stack, the temperature effect of the solder layers was not taken into account in the calculations. The results of the contact resistance calculations show that when using the standard process 1, the contact resistance is on average $3.6 \cdot 10^{-6}$ Ω·cm^2 and $2.7 \cdot 10^{-6}$ Ω·cm^2 for *p*- and *n*-type materials, respectively. For process 1, the accuracy of the contact resistance determination is consistent with the models and the results of measuring the cooling capacity of real coolers with leg lengths of 0.45 mm. Initial results for process 2 showed a significant decrease in the contact resistance. Namely, the contact resistances for *p*- and *n*-type materials were $1.1 \cdot 10^{-6}$ Ω·cm^2 and $1.3 \cdot 10^{-6}$ Ω·cm^2.

The maximum uncertainty in the contact resistance values does not exceed 20 %, which is good enough for determining contact resistances of the order of 10^{-6} Ω·cm^2. As the contact resistance decreases, the calculated value of ρ_c becomes more sensitive to variations in the figure of merit of the samples. Therefore, to measure contact resistances within $5 \cdot 10^{-7}$ Ω·cm^2, the samples should be pre-tested for a decrease in the standard deviation of the measured figure of merit values. One of the many advantages of this method is the ability to determine contact resistance over a wide temperature range, and Table 1 shows the decrease in contact resistance with decreasing temperature, which clearly reflects the temperature dependence of volume resistances in accordance with "narrowing effects".

Conclusions

1. The most accurate method for measuring electrical contact resistance is the Kelvin method in its six-terminal modification. This method is successfully used in microelectronics. There is no information in the literature about its application in thermoelectricity.
2. The only known method for measuring the contact resistance of soldered metal contacts to a thermoelectric material is a modified method based on measuring the figure of merit of a stack of TEM wafers with many contacts. This method needs improvement to reduce the error in measuring the contact resistance, which is 20%.

References

1. Cox R.H., Strack H. (1969). *Sol. St. Electron*., 12, 89.
2. Heime K., Konig U., Kohn E., Wortmann A. (1974). *Sol. St. Electron*., 17, 835.
3. Berger H.H. J. (1972). Electrochem. Soc., 119, 507.
4. Gutai L., Mojres T. Appl.Phys. Lett. (1975). 26, 325.
5. Misra P., Nagaraju J. (2004). Test facility for simultaneous measurement of electrical and thermal contact resistance. *Rev. Sci. Instr*., Aug.2004, doi 10.1063/1.1775316
6. Maheshappa N.D., Nagaraju J., Krishna Murthy N.V. (1998). A facility for electrical resistance contact measurement. *Rev. Sci. Instr*., Mar.1998, doi 10.1063/1.1148810
7. Deepak, Krishna H. (2007). Measurement of small specific contact resistance of metals with resistive semiconductors. *J. El. Mat*., 36(5), 598-605, doi 10.1007/s11664-007-0091-y
8. Maheshappa H.D., Nagaraju J., Krishna Murthy M.V. (1998). A facility for electrical resistance contact measurement. *Rev. Sci. Instr*., Mar. doi 10.1063/1.1148810
9. Holgate T.C., Han L., Wu NY, Bojesen E.D., Cristensen M., Iversen Bo.B., Nong N.V., Pryds N. *Characterization of the interface between Fe-Cr alloy and the p-type thermoelectric oxide* $Ca_3Co_4O_9$.
10. Schroder D.K. (2006). *Semiconductor material and device characterization.* IEEE press. A John Wiley & Sons, Inc. Publication.
11. Gupta R.P., McCarty R., Sharp J. (2013). Practical contact resistance measurement method for bulk Bi_2Te_3 based thermoelectric devices. *J. El. Mat*.

Submitted 12.01.2022.

Вихор Л.М., *доктор фіз.-мат. наук* [1]
Горський П.В., *доктор фіз.-мат. наук* [1,2]
Лисько В.В., *канд. фіз.-мат. наук* [1,2]

[1] Інститут термоелектрики НАН та МОН України,
вул. Науки, 1, Чернівці, 58029, Україна;
[2] Чернівецький національний університет імені Юрія Федьковича,
вул. Коцюбинського 2, Чернівці, 58012, Україна
e-mail: anatych@gmail.com

МЕТОДИ ВИМІРЮВАННЯ КОНТАКТНИХ ОПОРІВ СТРУКТУР «МЕТАЛ – ТЕРМОЕЛЕКТРИЧНИЙ МАТЕРІАЛ» (ЧАСТИНА 1)

Наведено огляд існуючих методів вимірювання електричного контактного опору. Проведено аналіз їх точності, переваг та недоліків, а також можливостей використання у термоелектриці для дослідження та оптимізації структур «метал – термоелектричний матеріал». Бібл. 11, рис. 14.

Ключові слова: електричний контактний опір, вимірювання, точність, термоелектричні перетворювачі енергії.

Література

1. Cox R.H., Strack H. (1969). *Sol. St. Electron*., 12, 89.
2. Heime K., Konig U., Kohn E., Wortmann A. (1974). *Sol. St. Electron*., 17, 835.
3. Berger H.H. J. (1972). Electrochem. Soc., 119, 507.
4. Gutai L., Mojres T. Appl.Phys. Lett. (1975). 26, 325.
5. Misra P., Nagaraju J. (2004). Test facility for simultaneous measurement of electrical and thermal contact resistance. *Rev. Sci. Instr*., Aug.2004, doi 10.1063/1.1775316
6. Maheshappa N.D., Nagaraju J., Krishna Murthy N.V. (1998). A facility for electrical resistance contact measurement. *Rev. Sci. Instr*., Mar.1998, doi 10.1063/1.1148810
7. Deepak, Krishna H. (2007). Measurement of small specific contact resistance of metals with resistive semiconductors. *J. El. Mat*., 36 (5), 598 – 605, doi 10.1007/s11664-007-0091-y
8. Maheshappa H.D., Nagaraju J., Krishna Murthy M.V. (1998). A facility for electrical resistance contact measurement. *Rev. Sci. Instr*., Mar. doi 10.1063/1.1148810
9. Holgate T.C., Han L., Wu NY, Bojesen E.D., Cristensen M., Iversen Bo.B., Nong N.V., Pryds N. *Characterization of the interface between Fe-Cr alloy and the p-type thermoelectric oxide* $Ca_3Co_4O_9$.
10. Schroder D.K. (2006). *Semiconductor material and device characterization.* IEEE press. A John Wiley & Sons, Inc. Publication.
11. Gupta R.P., McCarty R., Sharp J. (2013). Practical contact resistance measurement method for bulk Bi_2Te_3 based thermoelectric devices. *J. El. Mat*.

Надійшла до редакції: 12.01.2022.